

Article

# Antioxidant and Anti-Colorectal Cancer Properties in Methanolic Extract of Mangrove-Derived *Schizochytrium* sp.

Kaliyamoorthy Kalidasan <sup>1,\*</sup>, Laurent Dufossé <sup>2,\*</sup>, Gunasekaran Manivel <sup>3</sup>, Poomalai Senthilraja <sup>3</sup> and Kandasamy Kathiresan <sup>4</sup>

<sup>1</sup> Atal Centre for Ocean Science and Technology for Islands, National Institute of Ocean Technology, Dollygunj, Port Blair 744103, Andaman and Nicobar Islands, India

<sup>2</sup> Chemistry and Biotechnology of Natural Products, CHEMBIOPRO, Université de La Réunion, ESIROI Agroalimentaire, 15 Avenue René Cassin, CS 92003, CEDEX 9, F-97744 Saint-Denis, Ile de La Réunion, France

<sup>3</sup> Department of Bioinformatics, Bharathidasan University, Trichy 620024, India; gmaniinfo07@gmail.com (G.M.); lionbioinfo@gmail.com (P.S.)

<sup>4</sup> Faculty of Marine Sciences, Annamalai University, Parangipettai 608502, India; kathiresan57@gmail.com

\* Correspondence: marinedasan87@gmail.com (K.K.); laurent.dufosse@univ-reunion.fr (L.D.); Tel.: +91-9965262514 (K.K.); +33-262217544 (L.D.)

**Abstract:** This work studied the antioxidant and anti-colorectal cancer properties of a potential strain of thraustochytrids, *Schizochytrium* sp. (SMKK1), isolated from mangrove leaf litter. The biomass was extracted with methanol and screened for antioxidant activity using six different assays. The extract exhibited the highest total antioxidant activity ( $87.37 \pm 1.22\%$ ) and the lowest nitric oxide radical ( $75.12 \pm 2.22\%$ ), and the activity increased with the concentration of the extract. The methanolic extract was further tested for in vitro cytotoxicity on the colon cancer cell line (HT29). The extract was also analyzed for polyunsaturated fatty acids using GC-MS. The five predominant HTVS-based compounds, viz., arachidonic acid, linolenic acid (alpha-linolenic acid and gamma-linolenic acid), eicosapentaenoic acid, and docosahexaenoic acid, were identified in the extract, and these were tested against the colon cancer protein IGF binding (IGF-1) using the in silico docking method. The results revealed that all the five compounds were capable of destroying the colon oncoprotein responsible for anti-colon carcinogen, based on activation energy and also good hydrogen bond interaction against IGF binding proteins. Of the compounds, docosahexaenoic acid was the most effective, having a docking score of  $-10.8$  Kcal/mol. All the five fatty acids passed the ADMET test and were hence accepted for further clinical trials towards the development of anticancer drugs.

**Keywords:** mangrove; thraustochytrid; *Schizochytrium*; PUFA; antioxidant; anti-colon cancer activity



**Citation:** Kalidasan, K.; Dufossé, L.; Manivel, G.; Senthilraja, P.; Kathiresan, K. Antioxidant and Anti-Colorectal Cancer Properties in Methanolic Extract of Mangrove-Derived *Schizochytrium* sp. *J. Mar. Sci. Eng.* **2022**, *10*, 431. <https://doi.org/10.3390/jmse10030431>

Academic Editor: Azizur Rahman

Received: 3 January 2022

Accepted: 11 March 2022

Published: 16 March 2022

**Publisher's Note:** MDPI stays neutral with regard to jurisdictional claims in published maps and institutional affiliations.



**Copyright:** © 2022 by the authors. Licensee MDPI, Basel, Switzerland. This article is an open access article distributed under the terms and conditions of the Creative Commons Attribution (CC BY) license (<https://creativecommons.org/licenses/by/4.0/>).

## 1. Introduction

Cancer is an abnormal growth of cells caused by oncoprotein activation or genes suppressing tumors that lead to alterations in cell function [1]. Cancer is a group of diseases in which abnormal cells spread and multiply uncontrollably. If the proliferation of these abnormal cells is not arrested, death is ultimately a great possibility. The present diet and lifestyle of consuming a high amount of meat and extreme alcohol use, along with less physical activity, have led to increasing deaths due to cancer. By 2030, approximately 21.4 million cancers will arise globally, and 13.2 million of these diseases are expected to cause death. Cancer accounts for 1 in every 6 deaths worldwide [2].

Colon cancer is one of the most dangerous types of cancer because it can spread to the lung, liver, ovaries, and other gastrointestinal organs. Colorectal cancer (CRC) is the third most common cancer affecting both men and women around the world, and it tends to increase with age [3–5]. Colorectal cancer rates are the highest in black men and women [6]. About 96% of colorectal cancers are adenocarcinomas that begin in the cells of the gland that make mucus lubricate the colon and rectum [7]. Numerous studies have

demonstrated the over expression of Insulin-like growth factors (PDB ID: 2DSQ). IGF plays a very imperative role in colorectal cancer. The insulin-like growth factor (IGF) system consists of the peptide growth factors IGF-I and IGF-II, the type I and II IGF receptors, the IGF-binding proteins (IGFBP), and their corresponding proteases [2,8]. Initially identified as potent physiological mitogens, IGF are now known to be polypeptides with effects on cell proliferation, differentiation, apoptosis, and transformation [3,9]. Colon cancer is one of the most frequent malignant diseases in the developed world, and experimental and clinical data implicate the IGFIR in colon cancer etiology. Compared with normal tissues, the IGF-IR is overexpressed by tumors in colorectal cancer [10,11]. In addition, IGF-I protects colon cancer cells from death factor-induced apoptosis [12]. Furthermore, IGF-II mRNA is overexpressed in human colon carcinoma compared with normal adjacent tissues [13]. Therefore, the discovery of agents that inhibit the IGF-I signaling pathway could lead to the development of highly successful prevention strategies for colon cancer.

Marine organisms are a wealthy source of structurally novel and biologically active metabolites [14]. To date, many marine compounds with various biological functions have been discovered and only a few of them are under investigation for development as new drugs [15,16].

Thraustochytrids are obligate marine microorganisms with a diverse group of marine osmoheterotrophic fungi-like stramenopile protists. They belong to the eukaryotic kingdom of stramenopiles, which includes oomycetes and diatoms [17,18]. They could be a potential source of omega-3 polyunsaturated fatty acids (PUFAs) such as docosahexaenoic acid (DHA) and eicosapentaenoic acid (EPA) for commercial production [19–21]. Thraustochytrids are being studied as a supplement for the production of animal feed [22], biodiesel [23], enzymes [24], squalene [25], antimicrobials [19–21], antioxidants [20,26], exopolysaccharides [27], vaccines [28], nanoparticles [20], and haemolytic (21) and anticancer drugs [29]. In addition to PUFAs, thraustochytrids contain some anti-oxidative pigments such as carotenoid and astaxanthin, which are linked to a lower risk of cancer through free-radical scavenging, lipid peroxidation reduction, and immune system activation [30]. There are no reports of thraustochytrids producing toxic chemical/compounds [31]. However, only a few studies have been conducted on the thraustochytrids from mangrove sources for their medicinal potential [19–21,32], and hence, the current research work was undertaken to study the antioxidant and anticancer potentials of thraustochytrids isolated from decomposing mangrove leaves.

## 2. Materials and Methods

### 2.1. Isolation and Culture Conditions of Thraustochytrids from Mangroves

Thraustochytrid strains were isolated from decaying mangrove leaf litter of *Rhizophora mucronata* Poir., collected from Pichavaram mangrove forest on the southeast coast of India by the pour plate technique on glucose yeast peptone agar medium (GYPA) prepared in natural seawater (NSW) (25 ppt) with the addition of antifungal (fluconazole  $100 \mu\text{g}\cdot\text{L}^{-1}$ ) and antibacterial (streptomycin  $100 \mu\text{g}\cdot\text{L}^{-1}$ ) agents to prevent bacterial and fungal contamination, and they were incubated at  $28^\circ\text{C}$  and pH 7.2 for 2–5 days [19–21,32]. After the incubation, white-to-pale-white colonies and oily colonies with smooth and rough surfaces were found. The pure isolates were obtained after sub-culturing 3 times every 2–5 days and kept on agar slants at  $4^\circ\text{C}$  until further use and sub-cultured every month [19–21,32]. The predominant strains were chosen for morphological and molecular (18S rDNA) identifications.

### 2.2. Morphological Identification of Thraustochytrids

Morphological identification of thraustochytrid isolates was carried out under a light microscope (LM) based on colony color, size, shape, zoospore production, amoeboid cells, vegetative cells, and presence of the ectoplasmic network. Pure colonies of thraustochytrid isolates were taken from the culture medium by sterile metal loops and these were stained with acriflavine at a concentration of  $0.02 \mu\text{g}\cdot\text{mL}^{-1}$ . Further freeze-dried, gold coating

thraustochytrid cells were observed under a scanning electron microscope (SEM) using the standard methods [20,21].

### 2.3. DNA Extraction and Amplification of the 18S rDNA Gene

Genomic DNA of thraustochytrid isolates was extracted [20,32,33] by the method of Mo and Rinkevich. Briefly, 3 mL of 48–96-h-old thraustochytrid cell culture was centrifuged at 10,000 rpm (1.5 mL tubes) for 5 min at 4 °C. The cell pellets were resuspended in 200 µL of lysis buffer (0.25 M Tris-HCl (pH 8.2), 0.1 M EDTA, 2% Sodium Dodecyl Sulfate, and 0.1 M NaCl), and maintained at 55 °C for 30 min in a water bath. Chloroform–isoamyl alcohol (24:1) was used to extract DNA, which was then precipitated with ice-cold isopropanol. The extracted DNA was dissolved in 30 µL of TE buffer and stored at –20 °C for further use. The small subunit gene was amplified in a (Tech Gene™) thermal cycler using primers (18S001-5'-AACCTGGTTGATCCTGCCAGTA-3', 18S13-5'-CCTTGTTACGACTTCACCTTCCTCT-3') [34]. The amplification cycle involved an initial denaturation step of 94 °C for 60 s, followed by 35 cycles of (i) denaturation (94 °C for 60 s), (ii) annealing (50 °C for 60 s), and (iii) elongation (72 °C for 120 s), and a final elongation step at 72 °C for 10 min. The molecular weight was checked using a molecular marker (100 bp ladder) [20]. The amplicon product was tested in a 1.5% agarose gel.

### 2.4. Sequencing and Phylogenetic Analyses of 18S rDNA Gene

The purification of PCR products and DNA sequencing were performed through the high-throughput MegaBace sequencer (YAAZH XENOMICS, Coimbatore, India). The resulting sequences were trimmed based on the electropherogram peak clarities in the MEGA 6.0 program. Sequences with noisy peaks were omitted from the analysis. The percent similarity of the amplified 18S rDNA gene sequences was confirmed by the NCBI's BLAST program. To confirm the species identity, a higher percentage (95–100%) of similarity to the reference sequence was used and sequences were submitted to the GenBank database at the National Center for Biotechnology Information (NCBI) [35]. The CLUSTAL W Multiple Sequence Alignment Program was used to align and analyze the successfully sequenced rDNA region of thraustochytrids against the whole non-redundant NCBI GenBank database [36]. A phylogenetic tree was created using all the available thraustochytrid gene sequences as well as sequences determined in this study using the maximum likelihood method. Statistical analysis of 1000 bootstrap replicates was used to assess the species relationship. The genus *Labyrinthula* was used as the out-group to group the phylogenetic analyses [20].

### 2.5. Biomass Production and Extraction of Intracellular Specialized Metabolites

The fresh cultures of the thraustochytrid strain (SMKK1) were maintained by culturing them separately in 1 mL of glucose yeast extract peptone seawater (GYPS) medium. GYPS medium was inoculated into 100 mL of modified glucose yeast extract peptone-production broth medium consisting of NSW, glucose (10 g·L<sup>-1</sup>), yeast extract (10 g·L<sup>-1</sup>), peptone (1 g·L<sup>-1</sup>), monosodium glutamate (1 g·L<sup>-1</sup>), thiamine (0.2 g·L<sup>-1</sup>), with a pH of 7.12 ± 0.1, and maintained under the optimized conditions. Then, intracellular metabolites were extracted from the biomass of thraustochytrid strain (SMKK1) [32]. The fresh biomass was rinsed with sterile double distilled water, extracted thrice with 80% methanol as solvent, and then left in a separating funnel for 15 min for precipitation. The crude extract was then filtered via Whatman No.1 filter paper, and the filtrate was dried under a vacuum desiccator at 40 °C.

### 2.6. Antioxidant Assays

The biomass of thraustochytrids strain (SMKK1) extracted with methanol in different concentrations of 50, 100, 150, 200, and 250 µg·mL<sup>-1</sup> was tested for antioxidant activity using standard assay methods for total antioxidant activity [20], DPPH radical scavenging [20], reducing power [37], hydrogen peroxide radical inhibition [38,39], nitric oxide

radical inhibition [38,40], and total phenol content [41]. L-Ascorbic acid was used as a positive control, and all the experiments were conducted in triplicate.

### 2.7. GC-MS Analysis (Gas Chromatography-Mass Spectroscopy)

Total lipids of the thraustochytrid strain (SMKK1) biomass were estimated using the method of Folch et al. [42]. Fatty acid methyl ester (FAME) prepared from the lipid was analyzed using gas chromatography-mass spectroscopy (GC-MS) for the identification of various fatty acids [43,44]. In brief, 2  $\mu$ L of the extract was immediately injected through the FID and Heliflex AT-225 capillary column of GC-MS equipped with a mass detector, Turbo mass gold Perkin-Elmer with an Elite-5MS, and helium as transporter gas. The detector temperature was 280 °C, while the injector temperature was 250 °C. Temperature programming ranged from 200 °C at 10 °C/min without holding up to 280 °C at 5 °C/min with 9 min of holding. Nitrogen was used as a transporter gas at a pressure of 6 psi. After analysis, peaks were identified and quantified with the known compound MS Library [45]. The compound structures were retrieved from the PubChemBioAssay database (<http://pubchem.ncbi.nlm.nih.gov>, accessed on 3 July 2021).

### 2.8. Preparation of Protein and Ligand Structures

The X-ray crystallographic structure of the IGF binding (IGF-1) protein receptor (PDB I.D: 2DSQ) was downloaded from the Protein Data Bank (PDB) (<http://www.rcsb.org/pdb/>, accessed on 2 January 2022). The water molecules were extracted from the protein coordinate file 1NAV before docking. Energy minimization was conducted by applying the Chemistry at Harvard Macromolecular Mechanics (CHARMM) force field. Chemical compounds derived from the thraustochytrid strain (SMKK1) were identified by GC-MS. The compound structures were retrieved from the PubChem online server and generated from Simplified Molecular Input Line Entry Specification (SMILES) notation using ChemSketch Software (CS) ([www.acdlabs.com](http://www.acdlabs.com), accessed on 2 January 2022). The GCMS- identified (19) ligand molecules were screened using PyRx 0.8 software. The best five compounds were used as Molecular Docking analysis, three-dimensional optimizations were made, and then the MOL file was served.

### 2.9. Molecular Docking Analysis

The docking analysis was carried out to explore the interaction of the thraustochytrid strain (SMKK1)-derived fatty acids such as arachidonic acid (AA), linolenic acid (alpha-linolenic acid (ALA) and gamma-linolenic acid (GLA)), eicosapentaenoic acid (EPA), and docosahexaenoic acid (DHA) with colon cancer protein, as well as IGF binding (IGF-1) (PDB I.D: 2DSQ) using AutoDock Vina 1.2.0. The compounds or ligands were chosen based on Lipinski's rule of five using "Lipinski drug filters" (<http://www.scfbio-iitd.res.in/utility/LipinskiFilters.jsp>, accessed on 2 January 2022). The interaction between the binding pockets of target (IGF-1) colon cancer protein and the test compounds was assessed to find the active site of the target protein. The docking results were visualized using the Discovery Studio Visualizer (DSV) 2021.

### 2.10. In Silico ADME Predictions for Pharmacokinetic Properties

The pharmacokinetic properties of the polyunsaturated fatty acids were estimated using the FAF-Drugs3 server (<http://fafdrugs3.mti.univ-paris-diderot.fr>, accessed on 2 January 2022) [46]. For computational prediction, the ligand structural data were used in .sdf format, XLOGP3 was set as logP, and other parameters were set as default for computational prediction [47].

### 2.11. Determination of the In Vitro Anti-Proliferative Effect of Thraustochytrid Extracts on Colon Cell Lines

Colon cancer cell line (HT29 cell line) was purchased from NCCS, Pune, India, cultured in Dulbecco's modified Eagle's medium (DMEM) enhanced with 10% Fetal calf serum

(FCS), l-glutamine, streptomycin, gentamycin, and penicillin, and grown in 5% CO<sub>2</sub> at 37 °C in a humidified atmosphere in a CO<sub>2</sub> incubator. The effect of the thraustochytrid extract was tested on colon cancer cell lines as well as normal cell lines (VERO cell lines, African Green Monkey kidney cell lines). The DMEM was diluted in sterilized millipore double distilled water and thoroughly mixed before being sterilized at 15 lbs, 121 °C for 15 min. The contents were mixed well with shaking depending on the concentrations of fetal calf serum (2% or 10%) and the pH was adjusted to 7.2–7.4. The DMEM vials were kept at 37 °C for 48 h and stored in the refrigerator after checking for sterility, pH drop, and floating particles [48].

#### 2.12. Preparation of Thraustochytrid Extracts

A working concentration of 1 mg·mL<sup>-1</sup> was obtained by dissolving an aliquot of 0.05 mL of extract in 4.95 mL of DMSO. Before each experiment, the working concentration was freshly prepared and filtered through a 0.45-micron filter. A quantity of 500 µL of FCS-free DMEM was taken into 8 microcentrifuge tubes for each sample, and 5 mL of extract was made at a concentration of 1 mg·mL<sup>-1</sup>. The samples were syringe filtered with a 0.45 µm filter to remove impurities. Then, 500 µL of the working concentration of the sample was poured into the first Eppendorf tube and thoroughly mixed, and 500 µL of this volume was serially diluted from the first tube to the last tube to obtain the appropriate concentrations of the thraustochytrid extract.

#### 2.13. MTT Cytotoxicity Assay

The MTT assay refers to the 3-(4,5-dimethyl thiazol-2yl)-2,5-diphenyl tetrazolium bromide test [49,50]. After incubation, the medium was carefully removed from the wells for the MTT assay. Each well was rinsed 2–3 times with DMEM without FCS before being filled with 200 µL of MTT (5 mg/mL). For cytotoxicity testing, the plates were incubated in a 5% carbon dioxide (CO<sub>2</sub>) incubator for 6–7 h. Following the incubation period, 1 mL of DMSO was added to each well, stirred with a pipette, and incubated for 45 s. Assuming any viable cells were present, it showed formazan crystals in the wake of adding solubilizing reagent (DMSO) and purple color formation. The suspension was moved to a spectrophotometer cuvette, and the optical density reading was made at 595 nm in a microplate reader (ELISASCAN, ERBA) using DMSO as a blank [51]. The standard graph was created by plotting the concentration of the extract on the X-axis and relative cell viability on the Y-axis.

$$\text{Cell viability (\%)} = \text{Mean OD/Control OD} \times 100$$

The cytotoxicity of the thraustochytrid extract and positive control in different concentrations of 3.9, 7.8, 15.6, 31.2, 62.5, 125, 250, 500, and 1000 µL·mL<sup>-1</sup> was tested on the cell line (HT29). The MTT assay was used to determine the viability of normal cell lines and the cell death of cancer cell lines after 24 h. As determined by the cell arrangement, the cells were also examined under a microscope, and microphotographs were taken. The IC<sub>50</sub> concentration was defined as the extract concentration that caused 50% cancer cell death, whereas the CC<sub>50</sub> concentration was defined as the extract concentration that caused 50% normal cell survival. As a positive control, doxorubicin was used. All the experiments were carried out in triplicates.

### 3. Results

#### 3.1. Morphological and Molecular Identification of Thraustochytrids

Based on the morphological characters, the predominant thraustochytrid strain (SMKK1) was identified as *Schizochytrium* sp. (displayed in Figure 1a), as indicated by their color, size, shape, and zoospore development, when seen under a light microscope at 40× brightening (Figure 1b). Further, the identity of the strain was confirmed through Scanning Electron Microscope (Figure 1c). In *Schizochytrium* sp., vegetative cells exhibited successive bipartition resulting in a cluster of cells, sporangium, and zoospores.

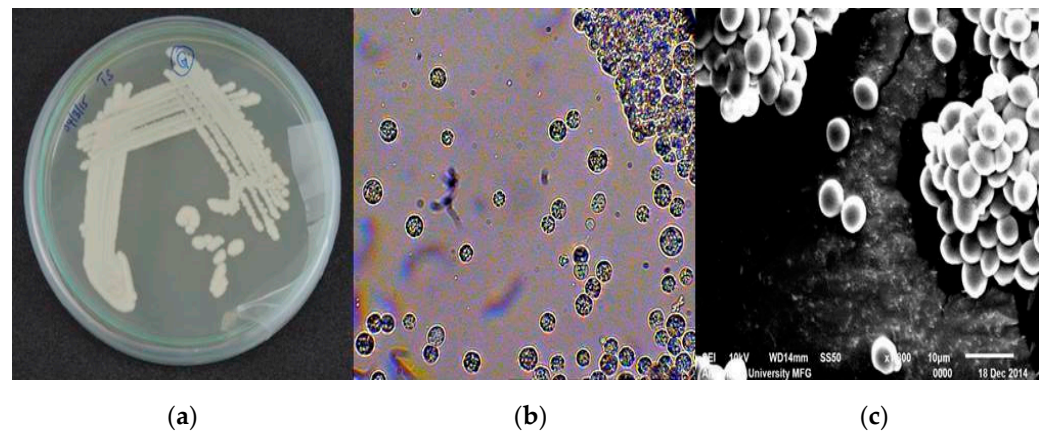


**Figure 1.** (a) Morphological, (b) light, and (c) scanning electron microscopic images of *Schizochytrium* sp. (SMKK1).

Further, the 18S region of rDNA from a marine thraustochytrid (SMKK1) was sequenced. According to NCBI BLAST analysis, the marine thraustochytrid strain *Schizochytrium* sp. (SMKK1) (Accession No. KT716338) was 99% closer to *Schizochytrium* sp. SW1 (KF500513). The blast results showed high 18S sequence similarity relative to other thraustochytrid strain sequences found in the GenBank database. The phylogenetic analyses confirmed the taxonomic position of the thraustochytrid species. Topologically, the phylogenetic tree consisted of two main clades, which were further subdivided into minor clades (Figure 2).

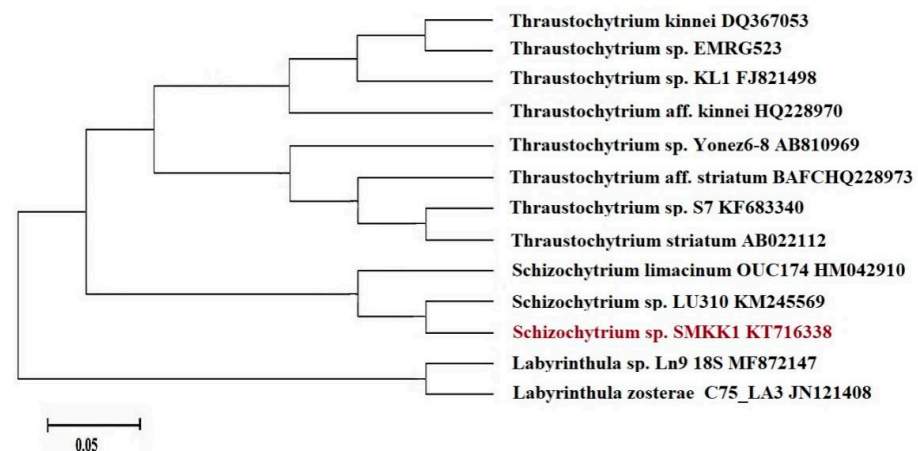


**Figure 2.** Neighbor-joining phylogenetic tree analysis of *Schizochytrium* sp. (SMKK1) with 18S rDNA gene sequence data.

### 3.2. Antioxidant Assay

The total antioxidant activity increased significantly with increasing concentrations of thraustochytrid extract ( $p < 0.05$ ). The extract exhibited the highest total antioxidant activity ( $87.37 \pm 1.22\%$ ), free radical scavenging activity ( $86.27 \pm 2.11\%$ ), total phenolic content ( $74.52 \pm 2.53\%$ ), hydrogen peroxide radical scavenging potential ( $78.23 \pm 2.47\%$ ), nitric oxide radical content ( $75.12 \pm 2.22\%$ ), and total reducing power ( $81.57 \pm 1.91\%$ ) (Figure 3).

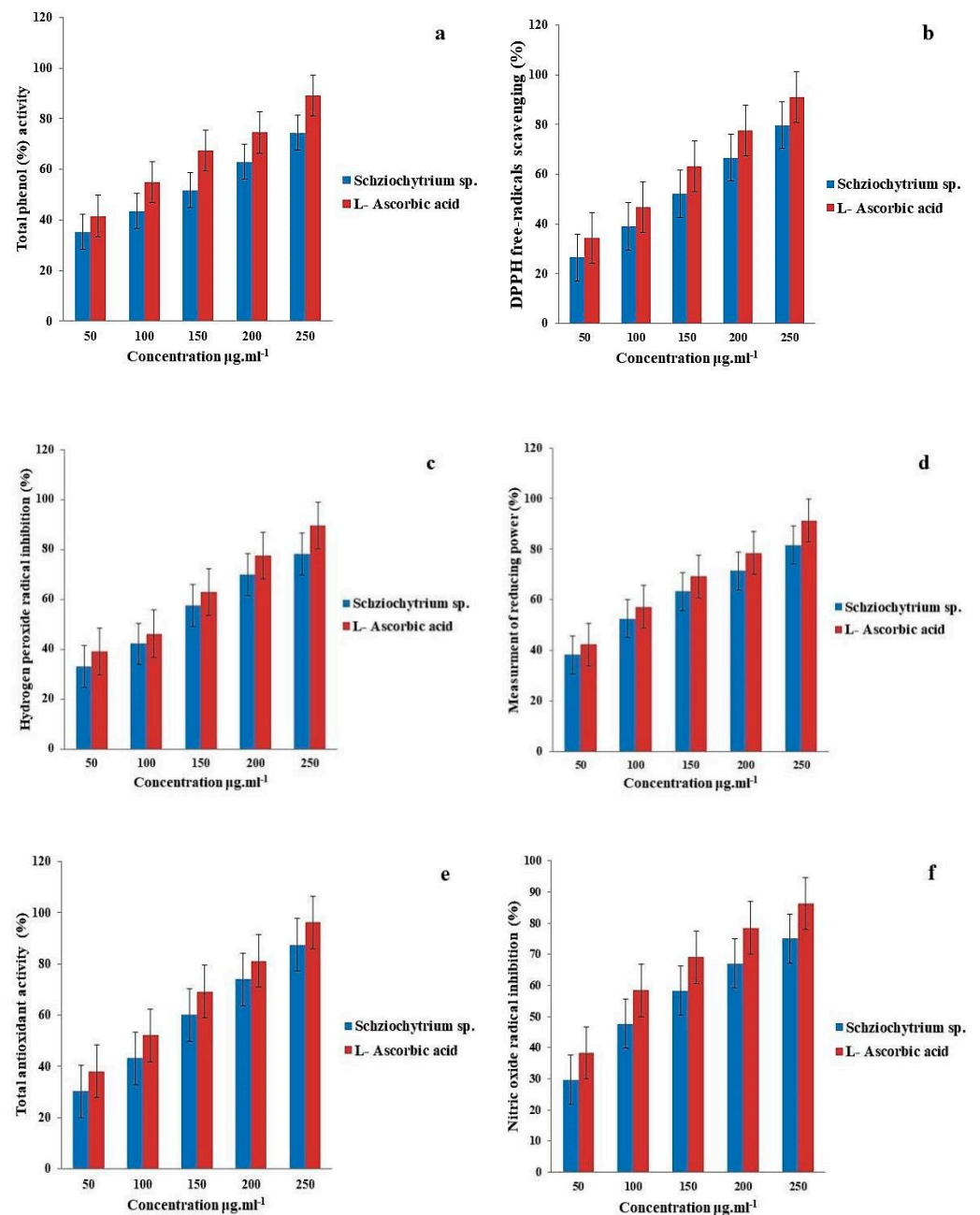


**Figure 3.** (a) Total phenol (%) content, (b) DPPH free-radicals scavenging (%) activity, (c) hydrogen peroxide radical inhibition (%), (d) total reducing power (%), (e) total antioxidant (%) activity, and (f) Nitric oxide radical inhibition (%) activity in different concentrations of the extract from *Schizochytrium* sp. (SMKK1).

### 3.3. Molecular Docking and ADME Predictions

The crude extract of *Schizochytrium* sp. (SMKK1) was analyzed by GC-MS. After analysis, peaks were identified and quantified with the known compounds using the MS Library (NIST Version-2005) (Table 1).

**Table 1.** Fatty acid composition of *Schizochytrium* sp. (expressed as % of the total fatty acids).

Compound S. No.	Carbon Atom of Fatty Acid	Name of the Fatty Acid	Content (%)
Comp 1	14:00	Methyl tetradecanoate acid	1.31 ± 0.18
Comp 2	14:01	Myristoleic acid	7.04 ± 1.21
Comp 3	15:00	Pentadecanoic acid	1.15 ± 0.13
Comp 4	16:00	Palmitic acid	37.32 ± 2.34
Comp 5	16:01	Palmitoleic acid	0.94 ± 0.11
Comp 6	17:00	Heptadecanoic acid	0.67 ± 0.14
Comp 7	18:00	Stearic acid	4.9 ± 0.72
Comp 8	18:01	Oleic acid	0.58 ± 0.11
Comp 9	18:2 n-6	Linolenic acid	0.41 ± 0.13
Comp 10	18:3 n-3	α-Linolenic acid	0.33 ± 0.08
Comp 11	18:3 n-6	γ-Linolenic acid	0.29 ± 0.10
Comp 12	18:04	Stearidonic acid	0.27 ± 0.07
Comp 13	20:00	Eicosanoic acid	0.38 ± 0.12
Comp 14	20:3 n-6	Dihomo-γ-linolenic acid	0.33 ± 0.14
Comp 15	20:4 n-3	Eicosatetraenoic acid	1.67 ± 0.25
Comp 16	20:4 n-6	Arachidonic acid	2.37 ± 0.57
Comp 17	20:5 n-3 (EPA)	Eicosapentaenoic acid	6.76 ± 1.08
Comp 18	22:5 n-6 (DPA)	Docosapentaenoic acid	1.22 ± 0.27
Comp 19	22:6 n-3 (DHA)	Docosahexaenoic acid	33.18 ± 2.16

Among the 19 identified compounds, five major polyunsaturated fatty acids, viz., arachidonic acid (AA), linolenic acid (LA), (alpha and gamma), eicosapentaenoic acid (EPA), and docosahexaenoic acid (DHA), were chosen for further study (Table 2). The 2D structures and properties of the fatty acids were generated by ChemSketch and 3D structures of them were visualized by Discover studio 4.0 (Figure 4) (Table 2) and were docked (PDB ID: 2DSQ) with IGF-1. The ligand fit of the docking analysis was carried out by AutoDock Vina 1.2.0. Virtualization was conducted using Discover studio 2021 (Biovia Dassaltun system v4.5 Software Inc., San Diego, CA, USA).

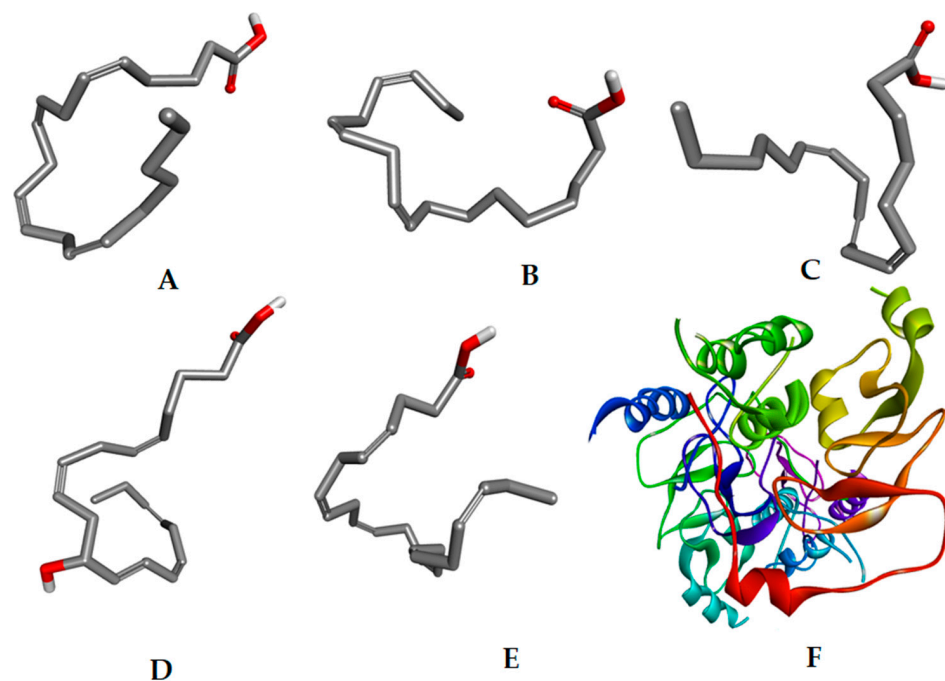


**Figure 4.** Three-dimensional structures of fatty acids: (A) arachidonic acid, (B) alpha-linolenic acid, (C) gamma-linolenic acid, (D) eicosapentaenoic acid, (E) docosahexaenoic acid, and (F) 3D Structure of IGF-1 complex (PDB ID: 2DSQ) obtained from the Protein Data Bank.

**Table 2.** Docking results of five selected PUFAs present in methanolic extract of *Schizochytrium* sp. strain SMKK1 against colon cancer protein.

S. No.	Compound Name	Molecular Formula	Molecular Weight (g/mol)	Hydrogen Donor and Acceptor	Docking Score Kcal/mol
Comp 10	Alpha-linolenic acid	C <sub>18</sub> H <sub>30</sub> O <sub>2</sub>	278.429	1, 2	−9.2
Comp 11	Gamma-linolenic acid	C <sub>18</sub> H <sub>30</sub> O <sub>2</sub>	278.429	1, 2	−9.0
Comp 16	Arachidonic acid	C <sub>20</sub> H <sub>32</sub> O <sub>2</sub>	304.466	1, 2	−8.0
Comp 17	Eicosapentaenoic acid	C <sub>20</sub> H <sub>30</sub> O <sub>2</sub>	302.451	1, 2	−9.7
Comp 19	Docosahexaenoic acid	C <sub>22</sub> H <sub>32</sub> O <sub>2</sub>	328.488	1, 2	−10.8

Arachidonic acid and IGF binding proteins produced five alkyl group amino acids (A:ARG:58, C:PHE:16, A: ARG:52, G:PRO:215, and A:CYS:53) and a strong hydrogen bond (A:ARG:28 and G:GLN:227) interaction while docking (Figure 5).

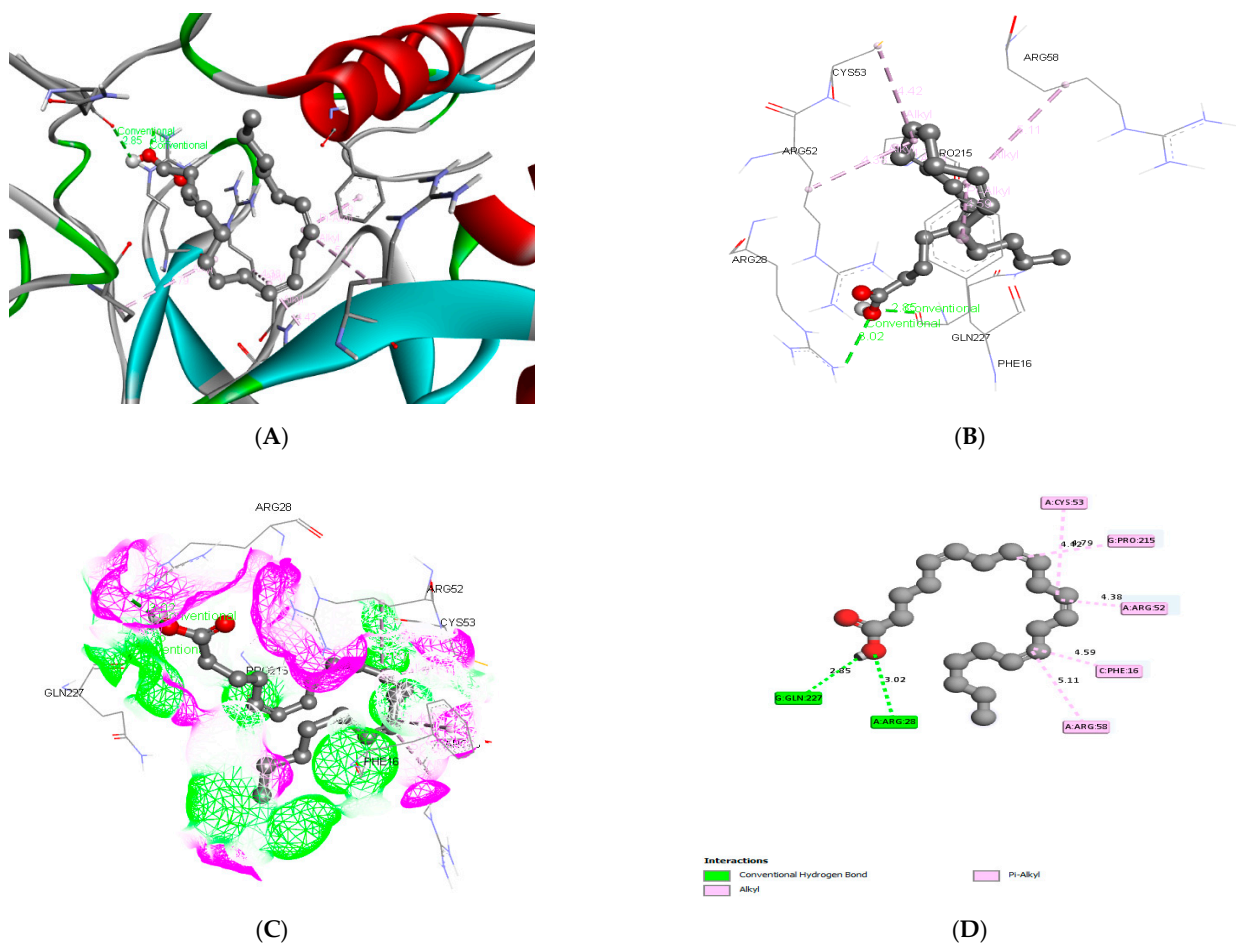


**Figure 5.** (A,B) Three-dimensional crystal structure with arachidonic acid (C) hydrogen surface created with selected compound and protein complex, and (D) 2D interactions between the target protein (2DSQ) and arachidonic acid. Green color interaction shows the hydrogen bond interaction.

Alpha-linolenic acid and IGF binding proteins produced alkyl group amino acids such as the Alkyl group of amino acids I:PHE:16, B:VAL:27, and B:ARGG:28, and the conventional hydrogen bond amino acid interaction while docking (Figure 6).

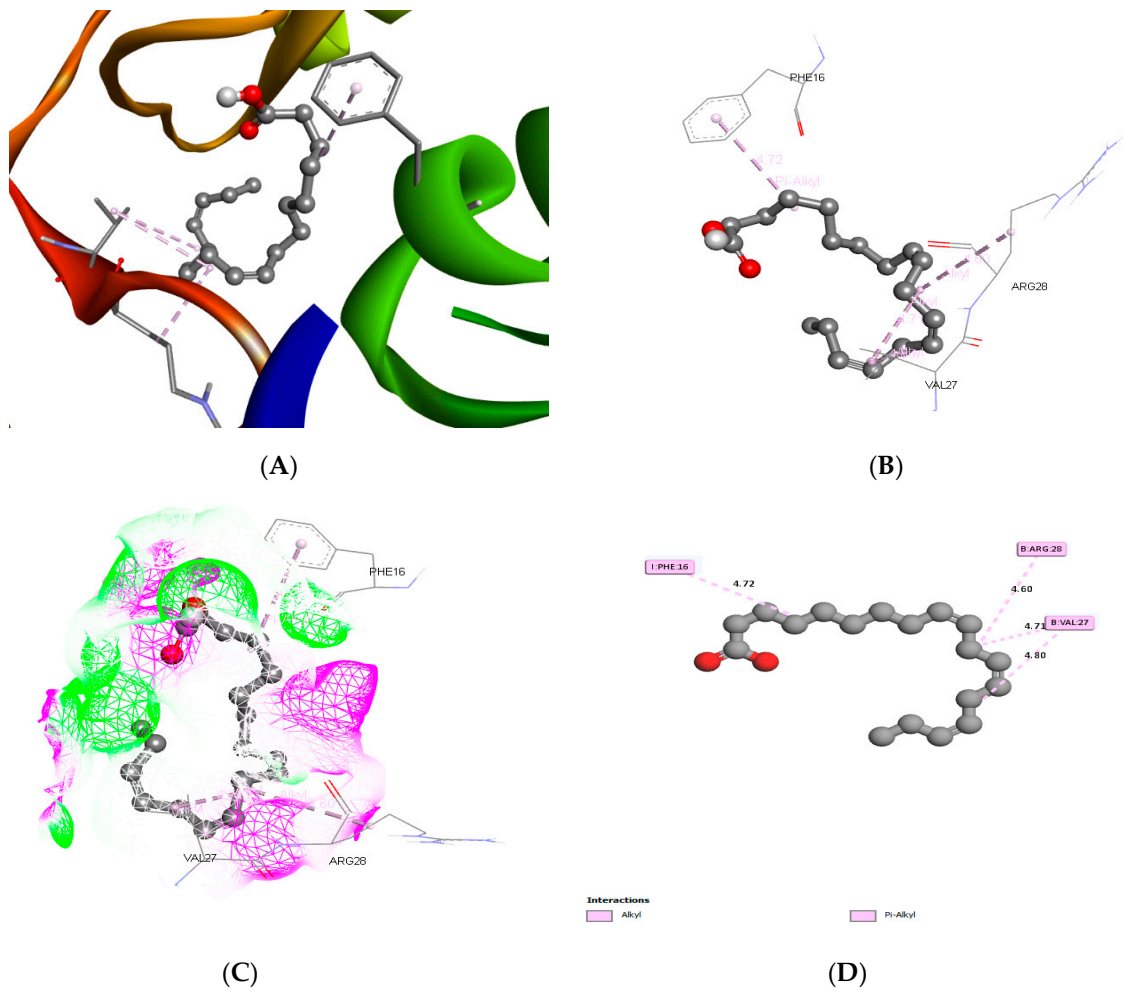


**Figure 6.** (A,B) Three-dimensional crystal structure with alpha-linolenic acid (C) hydrogen surface created with selected compound and protein complex, and (D) 2D interaction between the target protein (IGF-1) and Alpha-linolenic acid. Green color interaction shows the hydrogen bond interaction.

Gamma-linolenic acid and IGF binding proteins produced alkyl and pi-alkyl group amino acids such as B: CYS:59, I:PHE:16, B:CYS59, B:CYS:53, B:ARG:58, and B:LEU:82, one conventional hydrogen bond amino acid, and the attractive charge amino acid I:ASP:20 while docking (Figure 7).

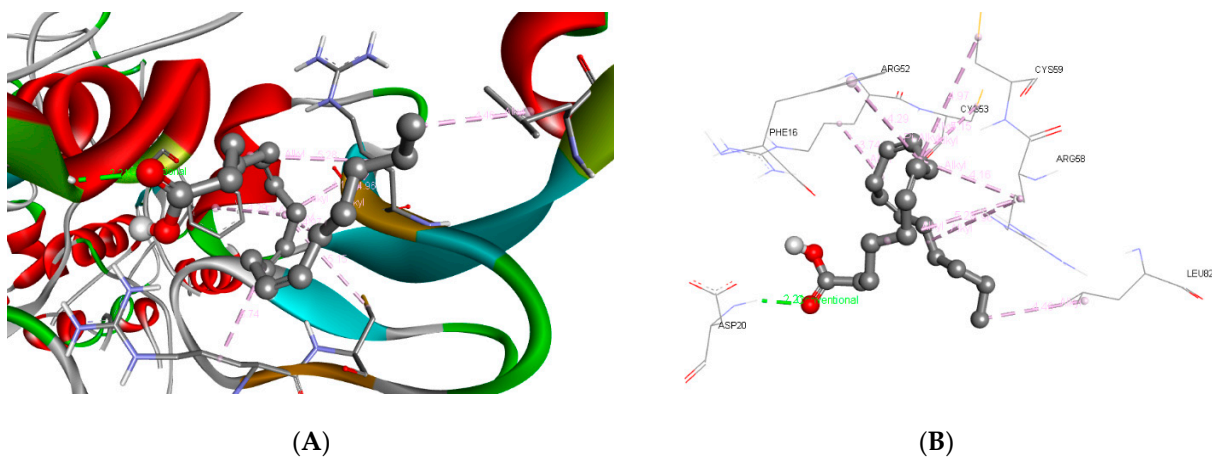


**Figure 7.** Cont.

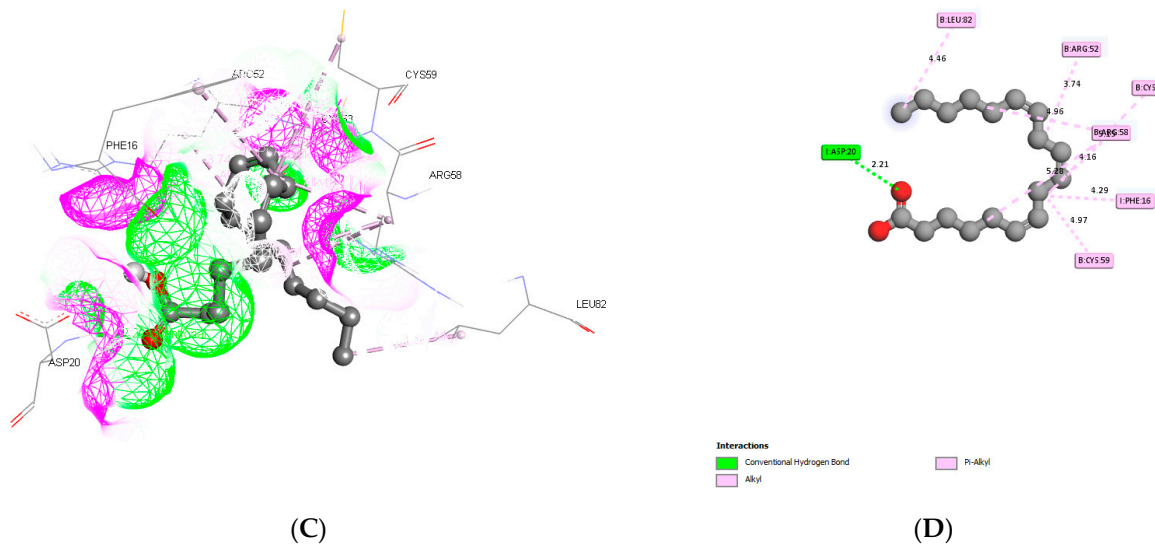


**Figure 7.** (A,B) Three-dimensional crystal structure with gamma-linolenic acid (C) hydrogen surface created with selected compound and protein complex, and (D) 2D interaction between (IGF-1) and gamma-linolenic acid. Green color interaction shows the hydrogen bond interaction.

While docking, eicosapentaenoic acid’s interaction with IGF binding proteins produced alkyl group amino acids such as A:CYS:53, C:PHE:16, A:ARG:58, A:GLY:56, A:LEU:57, G:PRO:215, and I:ASP:20, and the Pi-anion amino acids A:ARG:52 and C:ASP:20 (Figure 8).

Docosahexaenoic acid’s interaction with the (IGF-1) binding protein structure produced the conventional carbon bonds A:ARG:58, A:CYS:53, A:ARG:52, C:PHE:16, and G:PRO:215 and the hydrogen group amino acids A:LEU:57, A:GLY:56, and C:ASP:20 while docking (Figure 9).

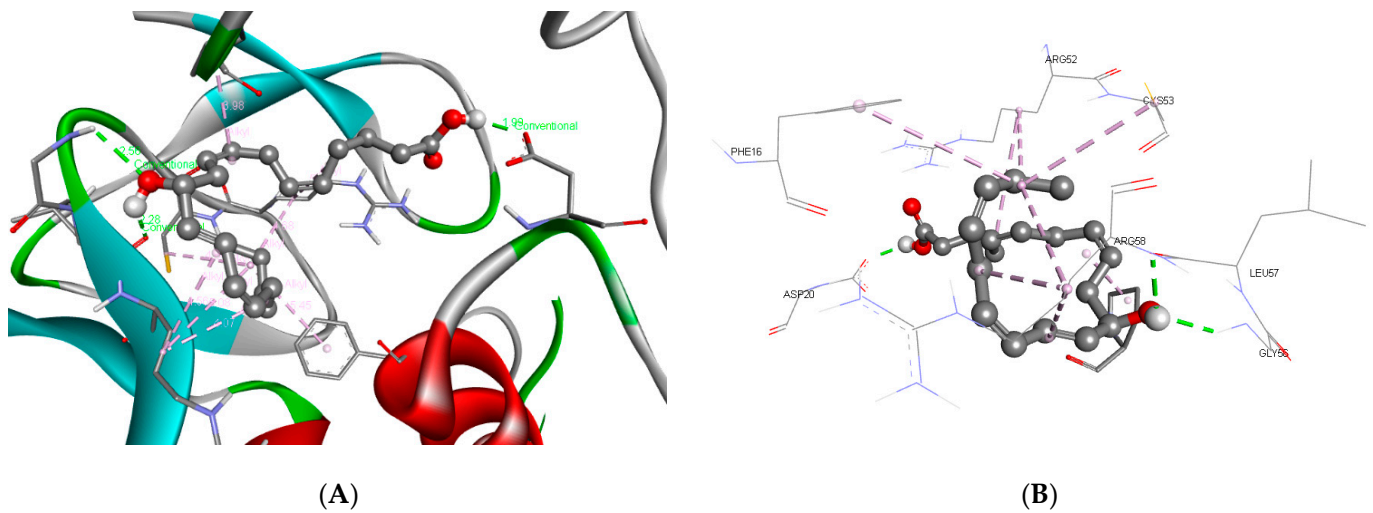


**Figure 8.** Cont.

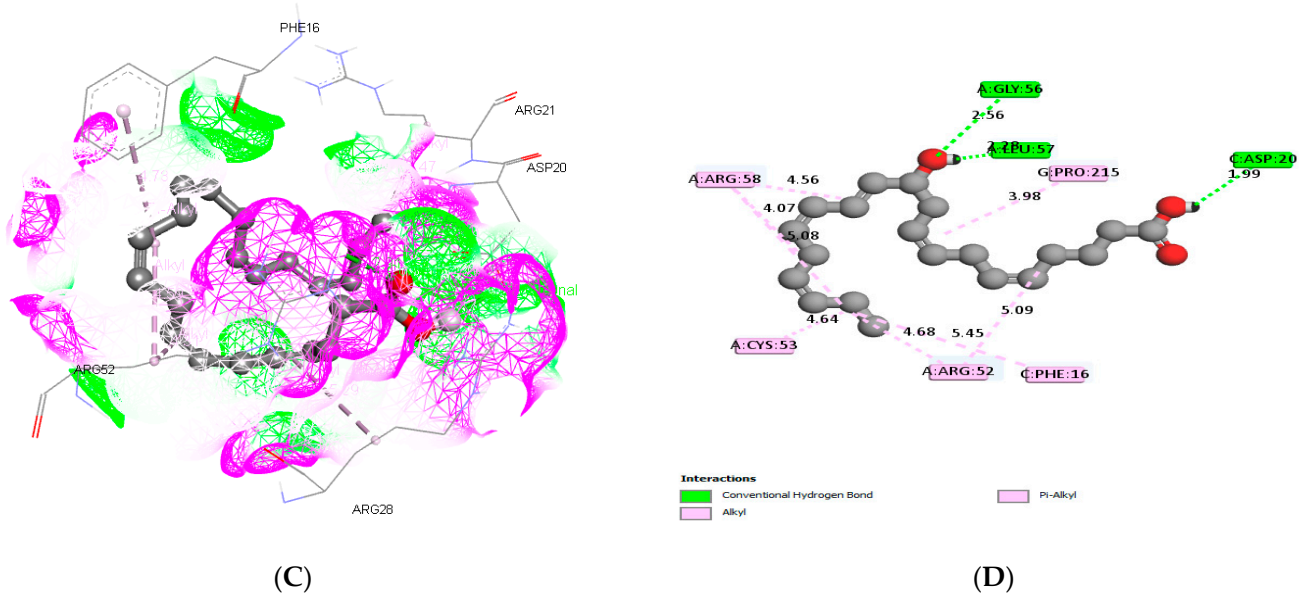


**Figure 8.** (A,B) Three-dimensional crystal structure with eicosapentaenoic acid (C) hydrogen surface created with selected compound and protein complex, and (D) 2D interaction between the target protein (IGF-1) and eicosapentaenoic acid. Pink color interaction shows the hydrophobic interaction.

The target protein was involved in ligand fit docking and produced bond formation with different amino residues in binding pockets, as well as producing bond formation with the IGF binding protein’s binding pocket amino acid, and the LibDock score values were  $-8.0$  for arachidonic acid,  $-9.2$  for alpha-linolenic acid,  $-9.0$  for gamma-linolenic acid,  $-9.7$  for eicosapentaenoic acid, and  $-10.8$  for Docosahexaenoic acid with IGF binding proteins (Table 2). The hydrogen bond and hydrophobic and aromatic interactions were created, the amino acid involved in the residues’ interaction in the binding gap for the five compounds was obtained, and the energy necessary for drug–receptor binding was directly correlated with the efficient binding of the compound. In this study, all fatty acids passed the ADMET test and were accepted for further clinical trials (Table 3).

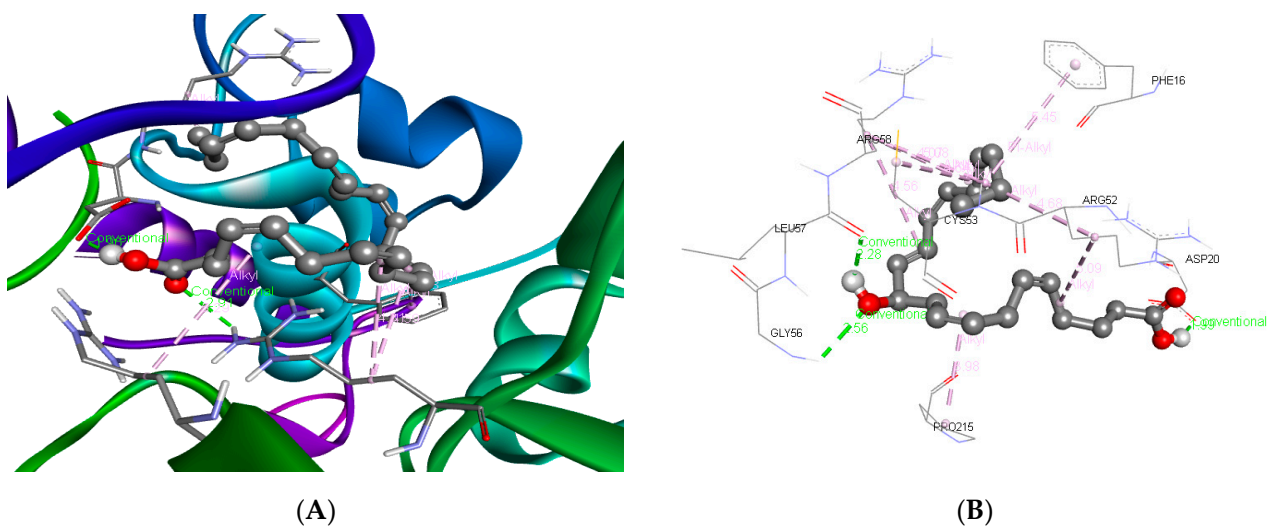


**Figure 9.** Cont.

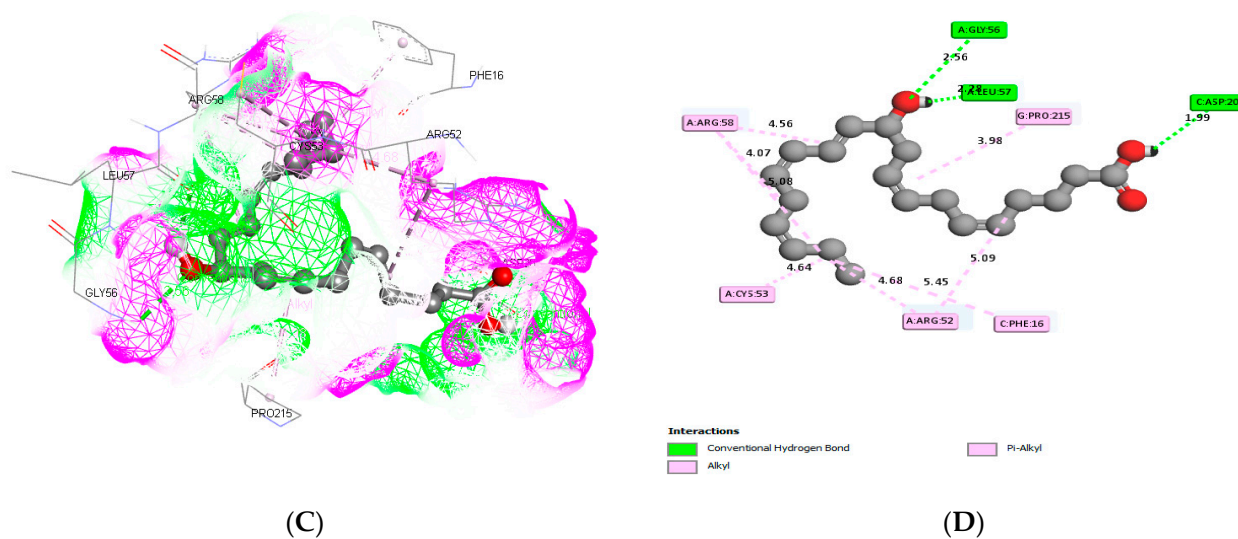


**Figure 9.** (A,B) Three-dimensional crystal structure with docosahexaenoic acid (C) hydrogen surface created with selected compound and protein complex, and (D) 2D interaction between the target protein (IGF-1) and Docosahexaenoic acid. Green color interaction shows the hydrogen bond interaction.

**Table 3.** ADMET screening of five selected PUFAs present in methanolic extract of *Schizochytrium* sp. strain SMKK1.

S. No.	Compound	MW	logP	logSw	HB Donors	HB Acceptors	Lipinski Violations	Solubility (mg/L)	Solubility	Oral Bio-Availability	Phospho Lipidosis	Status
Comp 10	AA	304.47	6.98	−5.2	1	2	1	1677.77	Good Solubility	Good	Non-Inducer	Accepted
Comp 11	ALA	278.43	6.46	−4.78	1	2	1	2342.23	Good Solubility	Good	Non-Inducer	Accepted
Comp 16	GLA	306.48	7.35	−5.38	1	2	1	1411.24	Good Solubility	Good	Non-Inducer	Accepted
Comp 17	EPA	302.45	6.29	−4.82	1	2	1	2440.06	Good Solubility	Good	Non-Inducer	Accepted
Comp 19	DHA	328.49	6.19	−4.85	1	2	1	2565.55	Good Solubility	Good	Non-Inducer	Accepted

### 3.4. In Vitro Colon Cancer Activity

The anti-cancer activity of *Schizochytrium* sp. (SMKK1) and positive control in different concentrations of 3.9, 7.8, 15.6, 31.2, 62.5, 125, 250, 500, and 1000  $\mu\text{L}\cdot\text{mL}^{-1}$  was tested by in vitro cytotoxicity against the colon cancer cell line (Figure 10). Cancer cell viability decreased with increasing thraustochytrid extract concentrations, and thus, the cell viability was concentration-dependent. The inhibitory concentration ( $\text{IC}_{50}$ ) value was 31  $\mu\text{g}\cdot\text{mL}^{-1}$  (Figure 11). The human colon cancer cell line (HT29) and the Vero cell line were seeded at a density of  $1 \times 10^5$  cells per well on a 96-well plate. After 24 h of inhibition, the samples were washed and visualized for morphological changes. The control plate did not show any morphological changes (Figure 12). The thraustochytrid extract inhibited the multiplication of colon cancer cells (HT29), as evidenced by the irregular joint aggregates with round and polygonal cell morphology (Figure 10).

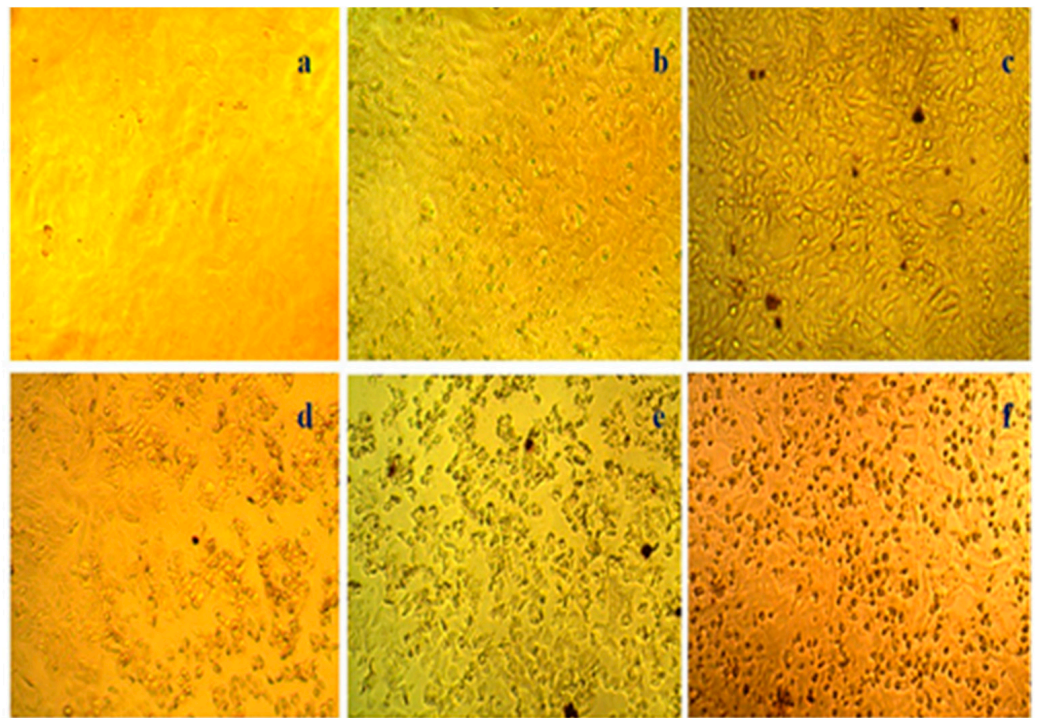


**Figure 10.** Effect of *Schizochytrium* sp. (SMKK1) extract on a colon cancer cell line (HT29): (a) untreated control cell, (b) cell treated with 3.9 µL/mL concentration, (c) cell treated with 15.6 µL/mL concentration, (d) cell treated with 62.5 µL/mL concentration, (e) cell treated with 250 µL/mL concentration, and (f) cell treated with 1000 µL/mL concentration.

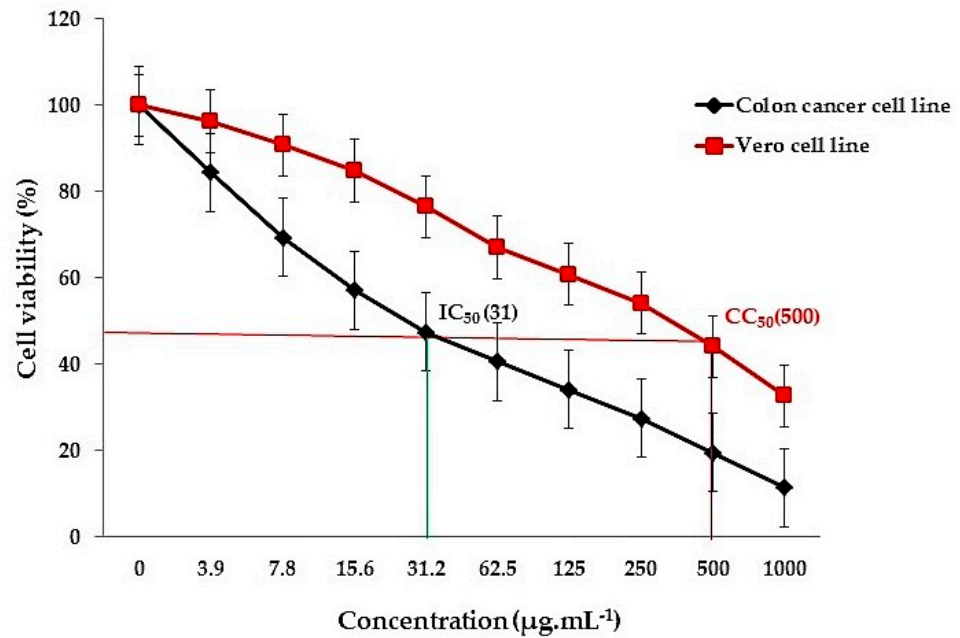


**Figure 11.** *Schizochytrium* sp. crude extract IC<sub>50</sub>, CC<sub>50</sub>, and therapeutic index values (SMKK1).

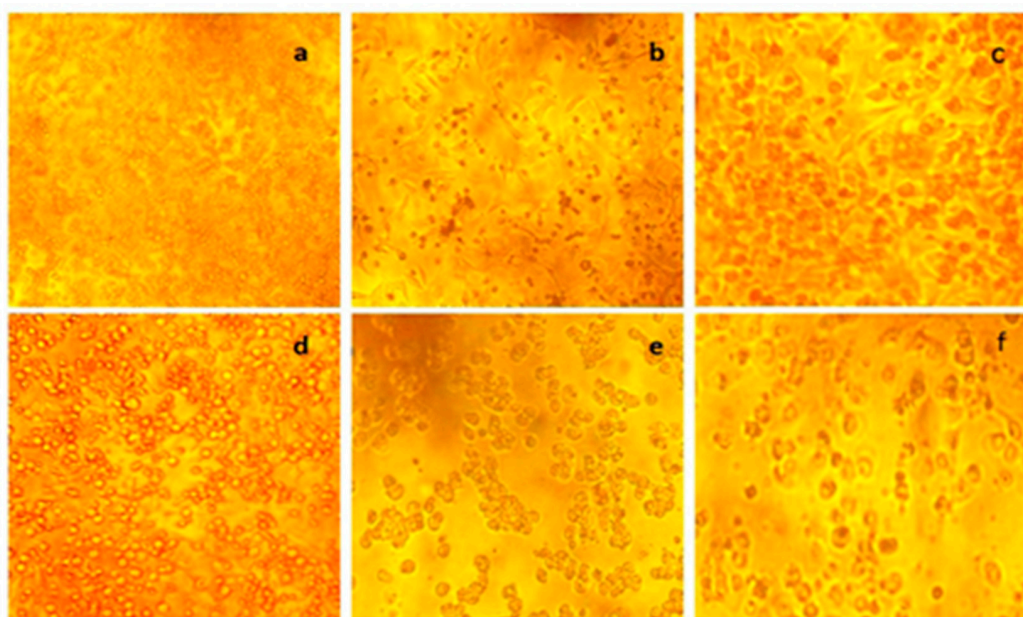


**Figure 12.** Effect of *Schizochytrium* sp. (SMKK1) extract on a normal Vero cell line: (a) untreated control cell, (b) 3.9  $\mu\text{L}/\text{mL}$  concentration-treated cell, (c) 15.6  $\mu\text{L}/\text{mL}$  concentration-treated cell, (d) 62.5  $\mu\text{L}/\text{mL}$  concentration-treated cell, (e) 250  $\mu\text{L}/\text{mL}$  concentration-treated cell, and (f) 1000  $\mu\text{L}/\text{mL}$  concentration-treated cell.

#### 4. Discussion

Thraustochytrids are generally non-motile (paraphyletic) in their assimilative phase [18]. In general, thraustochytrid taxonomy is based on morphology and life cycle-based studies [21,52,53]. A recent study described thraustochytrids in many monophyletic structures through morphology, biochemistry, and molecular information. Genera of *Aurantiochytrium*, *Botryochytrium*, *Monorhizochytrium*, *Oblongichytrium*, *Parietichytrium*, and *Sicyoidochytrium* were formed during the taxonomic revisions of *Schizochytrium* and *Ulkenia* [54–56].

Generally, identification of thraustochytrids at the species level is very difficult due to the morphological similarities between them, and many of the morphological characters used in their classification overlap with each other [17,21,57]. In this context, the importance of molecular techniques using 18S rDNA molecular sequences in understanding the classification of thraustochytrids is emphasized [34]. The taxonomy of thraustochytrids was later revised [54,55,58]. The phylogenetic analyses also confirmed the taxonomic positions of the thraustochytrid species. Topologically, the phylogenetic tree consists of two main branches that are further subdivided into smaller branches. The first clade mainly includes *Schizochytrium* sp., with a strong bootstrap value support of 100% [33]. However, molecular taxonomy is usually based on only one gene or protein and sometimes could be misleading. As a result, both morphology and whole-genome sequences are currently used to classify organisms.

The present study sequenced the 18S region of rRNA from thraustochytrids. Based on the NCBI BLAST analysis, the mangrove-derived thraustochytrid strain, *Schizochytrium* sp. (SMKK3) (Accession No. KT716338) was 99% closer to *Schizochytrium* sp. SW1 (KF500513). The blast results revealed a high similarity of the 18S sequence relative to other thraustochytrid sequences existing in the GenBank database. Moreover, the lack of reference gene sequence data in GenBank is also a significant disadvantage. This calls for and necessitates the use of both morphological and molecular gene identification of thraustochytrids. In addition, it is also recommended to use a multi-gene molecular approach for more reliable confirmation of the identity of the marine thraustochytrids.

Mangrove-derived thraustochytrids are the potential source of omega-3 polyunsaturated fatty acids (PUFAs) [19–21], as also evidenced in the present study that detected

the predominance of docosahexaenoic acids (DHA) and eicosapentaenoic acids (EPA) in *Schizochytrium* sp. (SMKK1) isolated from mangrove decaying leaf litter (Figure 1). This species displayed significant antioxidant activity with increasing concentrations of its extracts (Figure 2). The highest total antioxidant activity ( $87.37 \pm 1.22\%$ ) in the extract (Figure 3) could be attributed to the presence of polyunsaturated fatty acids in thraustochytrids as potential free-radical foragers [32,59]. Similar activity has also been reported in *Thraustochytrium kinnei* (TSKK1) and *Aurantiochytrium* sp. (ANVKK-06) [20,21].

Molecular docking is an important method for computer-based drug development for targeted diseases. Structural elucidation of compounds is conducted by GC-MS analysis. In the present study, GC-MS identified four major compounds, viz., arachidonic acid, linolenic acid (alpha and gamma), eicosapentaenoic acid, and docosahexaenoic acid (Table 1). An in silico High Throughput Virtual Screening (HTVS) and docking analysis was performed by docking 3D ligand molecules of the above-mentioned compounds with IGF binding (IGF-1) (PDB ID: 2DSQ) (Figure 4F), responsible for colorectal cancer.

The docked ligand molecules were chosen based on their docking energy and ability to interact with residues, as seen in Figures 5–9. The IGF binding proteins protein is used in a docking comparison with non-steroidal anti-inflammatory drugs [60]. The Libdock score values noted were  $-8.0$  for arachidonic acid,  $-9.2$  for alpha-linolenic acid,  $-9.0$  for gamma-linolenic acid,  $-9.7$  for eicosapentaenoic acid, and  $-10.8$  for docosahexaenoic acid with IGF binding proteins (Table 2). Lack of efficacy and safety are two major causes of drug failure, namely the absorption, distribution, metabolism, excretion, and toxicity (ADMET), and the chemical properties play an important role in all stages of drug discovery and development [61]. The probability of success or failure of a compound as drug can be arbitrated by the ADME-Tox prediction at the earlier stages, thereby avoiding costly late-stage processes [47,62]. In our study, all the tested fatty acids passed the ADMET test and were hence accepted for further clinical trials (Table 3).

The cytotoxicity effect of *Schizochytrium* sp. (SMKK1) extract on normal cell lines revealed that cell death occurred only at higher concentrations ( $500 \mu\text{g}\cdot\text{mL}^{-1}$ ) (Figure 10). The therapeutic index is a significant parameter as it incorporates anticancer activity and unavoidable toxicity to normal cells. This is the ratio between the concentration of the extract where 50% of cytotoxicity in the normal cell line occurs and the concentration of the test solution when 50% of cancer cell death occurs in the cancer cell line [63]. Drugs are considered for further testing only when the therapeutic index value is 16 or above. The present research work revealed a therapeutic index value of 16.12 for *Schizochytrium* sp. (SMKK1) extract against colon cancer, making it a potential drug candidate for further screening and purification processes (Figure 11). After inhibition, the cells were visualized for morphological changes. The control plate did not show any morphological changes (Figure 10), whereas the treated cells exhibited cell-damage-related reductions in cell volume and apoptotic bodies in a concentration-dependent manner (Figure 12).

PUFAs are promising molecules in the treatment of cancer diseases. The lipo-peroxidation is known to play a role in the anti-tumor effects of unsaturated fatty acids, particularly omega-3 polyunsaturated fatty [64]. The PUFAs, as well as C20-fatty acids such as arachidonic acid (AA) (C20:4), are strongly advocated for their inhibitory effect on the growth of cancer cells [65,66]. Eicosadienoic acid (C20:2) with linear-chain fatty acids is stronger in inhibiting cancer cells [67]. The  $\omega$ -3 fatty acids derived from fish, microalgae, and fungi are known to inhibit cancer by prompting the activity of enzymes and proteins associated with cell proliferation. A high intake of omega-6 PUFAs, omega-3 PUFAs, and omega-9 fatty acids has been experimentally proved to cure the cancers of the prostate, colon, and breast [68].

Docosahexaenoic acid (DHA) is known to suppress the proliferation of human cancer cells by 18–100% (SK-Mel-110 for malignant melanoma; MCF-7 for breast; HT-29 for colorectal; MHCC97L for Liver) [69]. SMKK1 inhibit the levels of IGF-1, thereby reducing carcinoma incidence and protecting against large intestine cancer. Consumption of a diet enriched with n-3 PUFAs (DHA), alpha-linolenic acids, arachidonic acid, and gamma-linolenic

acids could confer cardioprotective effects and anti-cancer activity against large intestine cancer [70]. Similarly, the present results revealed the cytotoxic activity of *Schizochytrium* sp. against the colon cancer (HT29) cell line. Moreover, there is no evidence of the thraustochytrids in producing poisonous compounds or causing diseases. Further purification of active compounds present in the extract of thraustochytrid species will provide potent lead compounds for developing anticancer drugs and nutraceuticals for human health.

## 5. Conclusions

The present study highlights the significance of *Schizochytrium* sp. (SMKK1), isolated from decomposing mangrove leaves, as a potential source of antioxidant and anti-colorectal cancer compounds. Nineteen compounds with a predominance of five polyunsaturated fatty acids were identified, using GC-MS, as being present in the methanolic extract of the thraustochytrid sp. All five polyunsaturated fatty acids were proven to have anti colon cancer activity by means of an in silico docking analysis with IGF binding (IGF-1) protein. The anti-colon cancer activity of the thraustochytrid species was further confirmed by cytotoxicity assay against colon cancer cell line (HT29) and by a high therapeutic index value of 16.12. This work emphasized the possible usage of *Schizochytrium* sp. (SMKK1) for further studies towards the development of an anticancer drug.

**Author Contributions:** K.K. (Kaliyamoorthy Kalidasan) designed the study, performed the laboratory experiments, prepared the original draft, performed the data analysis, and completed the writing, review, and editing of the manuscript; L.D. helped to design the study, and reviewed and edited the manuscript. G.M. and P.S. helped to design the study, wrote the methodology, and carried out the bioinformatics work. K.K. (Kandasamy Kathiresan) supervised the work and reviewed, edited, and approved the manuscript. All authors have read and agreed to the published version of the manuscript.

**Funding:** This research work was supported and funded by the Science and Engineering Research Board (SERB), New Delhi, under the National Postdoctoral Fellowship, PDF/2017/002579, dated 4 July 2018.

**Institutional Review Board Statement:** Not applicable.

**Informed Consent Statement:** Not applicable.

**Data Availability Statement:** Not applicable.

**Acknowledgments:** The authors are thankful for the DST-SERB fellowship, New Delhi (File Number: PDF/2017/002579) (K.K. (Kaliyamoorthy Kalidasan)) and UGC, New Delhi, for the BSR Faculty Fellowship (K.K. (Kandasamy Kathiresan)). Kaliyamoorthy Kalidasan thanks the authorities of ACOSTI-NIOT and Annamalai University, India, for providing the necessary facilities to carry out the project work. Laurent Dufossé is indebted to the Conseil Régional de La Réunion for continuous support in biotechnology research. We also thank Sunil Kumar Sahu, Beijing Genomics Institute (BGI-Shenzhen), Shenzhen, China, for assisting with the In Silico Pharmacokinetic Properties.

**Conflicts of Interest:** The authors declare no conflict of interest.

## References

1. Kopnin, B.P. Targets of oncogenes and tumor suppressors: Key for understanding basic mechanisms of carcinogenesis. *Biochemistry* **2000**, *65*, 2–27. [[PubMed](#)]
2. American Cancer Society. *Cancer Facts & Figures (2019)*; American Cancer Society: Atlanta, GA, USA, 2019.
3. Ferla, J.; Soerjomataram, I.; Ervik, M.; Dikshit, R.; Eser, S.; Mathers, C.; Rebelo, M.; Parkin, D.M.; Forman, D.; Bray, F. Cancer Incidence and Mortality Worldwide: Sources, Methods and Major Patterns in GLOBOCAN 2012. *Int. J. Cancer* **2015**, *136*, E359–E386. [[CrossRef](#)] [[PubMed](#)]
4. Arti, P. Genetic and environmental factors in cancer pathogenesis. *Int. J. Res.-Granthaalayah* **2015**, *3*, 2015.
5. American Cancer Society. *Colorectal Cancer Facts & Figures 2017–2019*; American Cancer Society: Atlanta, GA, USA, 2017.
6. Copeland, G.; Lake, A.; Firth, R. *Cancer in North America: 2006–2010. Volume One: Combined Cancer Incidence for the United States, Canada and North America*; North American Association of Central Cancer Registries, Inc.: Springfield, IL, USA, 2013.
7. Stewart, S.L.; Wike, J.M.; Kato, I.; Lewis, D.R.; Michaud, F. A population-based study of colorectal cancer histology in the United States, 1998–2001. *Cancer* **2006**, *107*, 1128–1141. [[CrossRef](#)] [[PubMed](#)]

8. Jones, J.I.; Clemmons, D.R. Insulin-like growth factors and their binding proteins: Biological actions. *Endocr. Rev.* **2009**, *16*, 3–34.
9. Baserga, R.; Hongo, A.; Rubini, M.; Prisco, M.; Valentini, B. The IGF-I receptor in cell growth, transformation and apoptosis. *Biochim. Biophys. Acta* **1997**, *1332*, F105–F126. [[CrossRef](#)]
10. Weber, M.M.; Fottner, C.; Liu, S.B.; Jung, M.C.; Engelhardt, D.; Baretton, G.B. Overexpression of the insulin-like growth factor I receptor in human colon carcinomas. *Cancer* **2002**, *95*, 2086–2095. [[CrossRef](#)]
11. Guo, Y.; Narayan, S.; Yallampalli, C.; Singh, P. Characterization of insulinlike growth factor I receptors in human colon cancer. *Gastroenterology* **2020**, *102*, 1101–1108. [[CrossRef](#)]
12. Remacle-Bonnet, M.M.; Garrouste, F.L.; Heller, S.; Andre, F.; Marvaldi, J.L.; Pommier, G.J. Insulin-like growth factor-I protects colon cancer cells from death factor-induced apoptosis by potentiating tumor necrosis factor alpha-induced mitogen-activated protein kinase and nuclear factor kappaB signaling pathways. *Cancer Res.* **2000**, *60*, 2007–2017.
13. Zhang, L.; Zhou, W.; Velculescu, V.E.; Kern, S.E.; Hruban, R.H.; Hamilton, S.R.; Vogelstein, B.; Kinzler, K.W. Gene expression profiles in normal and cancer cells. *Science* **1997**, *276*, 1268–1272. [[CrossRef](#)]
14. Ravikumar, S.; Kathiresan, K. *Marine Pharmacology Published by School of Marine Sciences; Alagappa University; Karaikudi, India*, 2010; p. 215.
15. Kim, S.K. *Marine Pharmacognosy: Trends and Applications*; CRC Press: New York, NY, USA, 2013.
16. Najafian, L.; Babji, A.S. A review of fish-derived antioxidant and antimicrobial peptides: Their production, assessment, and applications. *Peptides* **2012**, *33*, 178–185. [[CrossRef](#)] [[PubMed](#)]
17. Marchanan, F.L.; Chang, K.J.L.; Nichols, P.D.; Mitchell, W.J.; Polglase, J.L.; Gutierrez, T. Taxonomy, ecology and biotechnological applications of thraustochytrids: A Review. *Biotechnol. Adv.* **2017**, *36*, 26–46. [[CrossRef](#)] [[PubMed](#)]
18. Tsui, C.K.M.; Marshall, W.; Yokoyama, R.; Honda, D.; Lippmeier, J.C.; Craven, K.D.; Peterson, P.D.; Berbee, M.L. Labyrinthulomycetes phylogeny and its implication for the evolutionary loss of chloroplasts and gain of ectoplasmic gliding. *Mol. Phylogenet. Evol.* **2009**, *50*, 129–140. [[CrossRef](#)] [[PubMed](#)]
19. Kalidasan, K.; Sunil, K.S.; Kayalvizhi, K.; Kathiresan, K. Polyunsaturated fatty acid-producing marine thraustochytrids: A potential source for antimicrobials. *J. Coast. Life Med.* **2015**, *3*, 848–851.
20. Kalidasan, K.; Asmathunisha, N.; Gomathi, V.; Dufossé, L.; Kathiresan, K. Isolation and optimization of culture conditions of *Thraustochytrium kinnei* for biomass production, nanoparticle synthesis, antioxidant and antimicrobial activities. *J. Mar. Sci. Eng.* **2021**, *9*, 678. [[CrossRef](#)]
21. Kalidasan, K.; Vinitkumar, N.V.; Peter, D.M.; Dharani, G.; Dufossé, L. Thraustochytrids of mangrove habitats from Andaman Islands: Species diversity, PUFA profiles and biotechnological potential. *Mar. Drugs* **2021**, *19*, 571. [[CrossRef](#)]
22. Visudtiphole, V.; Phromson, M.; Tala, S.; Bunphimpapha, P.; Raweeratanapong, T.; Sittikankaew, K.; Arayamethakorn, S.; Preedanon, S.; Jangsutthivorawat, W.; Chaipayechara, S.; et al. *Aurantiochytrium limacinum* BCC52274 improves growth, hyposalinity tolerance and swimming strength of *Penaeus vannamei* post larvae. *Aquaculture* **2018**, *495*, 849–857. [[CrossRef](#)]
23. Chen, C.Y.; Lee, M.H.; Leong, Y.K.; Chang, J.S.; Lee, D.J. Biodiesel production from heterotrophic oleaginous microalga *Thraustochytrium* sp. BM2 with enhanced lipid accumulation using crude glycerol as alternative carbon source. *Bioresour. Technol.* **2020**, *306*, 123113. [[CrossRef](#)]
24. Bongiorno, L.; Pusceddu, A.; Danovaro, R. Enzymatic activities of epiphytic and benthic thraustochytrids involved inorganic matter degradation. *Aquat. Microb. Ecol.* **2005**, *41*, 299–305. [[CrossRef](#)]
25. Patel, A.; Liefeldt, S.; Rova, U.; Christakopoulos, P.; Matsakas, L. Co-production of DHA and squalene by thraustochytrid from forest biomass. *Sci. Rep.* **2020**, *10*, 1992. [[CrossRef](#)]
26. Kalidasan, K.; Sunil, K.S.; Narendran, R.; Kathiresan, K. Antioxidant activity of mangrove-derived marine thraustochytrids. *Mycosphere* **2015**, *6*, 602–611. [[CrossRef](#)]
27. Xiao, R.; Xi, Y.; Mi, L.; Xiang, L.; Yanzhang, W.; Min, C.; Arthur, R.; Mark, T.; Junhuan, D.; Yi, Z. Investigation of Composition, Structure and Bioactivity of Extracellular Polymeric Substances from Original and Stress-induced Strains of *Thraustochytrium striatum*. *Carbohydr. Polym.* **2018**, *195*, 515–524. [[CrossRef](#)] [[PubMed](#)]
28. Ramos-Vega, A.; Rosales-Mendoza, S.; Bañuelos-Hernández, B.; Angulo, C. Prospects on the Use of *Schizochytrium* sp. to Develop Oral Vaccines. *Front. Microbiol.* **2018**, *9*, 2506. [[CrossRef](#)] [[PubMed](#)]
29. Shakeri, S.; Amoozyan, N.; Fekrat, F.; Maleki, M. Antigastric cancer bioactive *Aurantiochytrium* oil rich in Docosahexaenoic acid: From media optimization to cancer cells cytotoxicity assessment. *J. Food Sci.* **2017**, *82*, 2706–2718. [[CrossRef](#)]
30. Atienza, G.A.M.V.; Arafiles, K.H.V.; Carmona, M.C.M.; Garcia, J.P.C.; Macabago, A.M.B.; Penacerrada, B.J.D.C.; Cordero, P.R.F.; Bennett, R.M.; Dedeles, G.R. Carotenoid analysis of locally isolated Thraustochytrids and their potential as an alternative fish feed for *Oreochromis niloticus* (Nile tilapia). *Mycosphere* **2012**, *3*, 420–428. [[CrossRef](#)]
31. Schmitt, D.; Tran, N.; Peach, J.; Edwards, T.; Greeley, M. Toxicologic evaluations of DHA-rich algal oil in rats: Developmental toxicity study and 3-month dietary toxicity study with an in utero exposure phase. *Food Chem. Toxicol.* **2012**, *50*, 4149–4157. [[CrossRef](#)]
32. Mo, C.; Rinkevich, B. A simple reliable and fast protocol for Thraustochytrid DNA extraction. *Mar. Biotechnol.* **2001**, *3*, 100–102. [[CrossRef](#)]
33. Honda, D.; Yokochi, T.; Nakahara, T.; Raghukumar, S.; Nakagiri, A.; Schaumann, K.; Higashihara, T. Molecular phylogeny of labyrinthulids and thraustochytrids based on the sequencing of 18S ribosomal RNA gene. *J. Eukaryot. Microbiol.* **1999**, *46*, 637–647. [[CrossRef](#)]

34. Tamura, K.; Stecher, G.; Peterson, D.; Filipinski, A.; Kumar, S. MEGA6: Molecular Evolutionary Genetics Analysis version 6.0. *Mol. Biol. Evol.* **2013**, *30*, 2725–2729. [CrossRef]
35. Thompson, J.D.; Higgins, D.G.; Gibson, T.J. CLUSTAL W: Improving the sensitivity of progressive multiple sequence alignment through sequence weighting, position-specific gap penalties and weight matrix choice. *Nucleic Acids Res.* **1994**, *22*, 4673–4680. [CrossRef]
36. Oyaizu, M. Studies on product of browning reaction prepared from glucose amine. *Jpn. J. Nutr.* **1986**, *44*, 307–315. [CrossRef]
37. Govindarajan, R.; Rastogi, S.; Vijayakumar, M.; Rawat, A.K.S.; Shirwaikar, A.; Mehrotra, S.; Pushpangadam, P. Studies on antioxidant activities of *Desmodium gangeticum*. *Biol. Pharm. Bull.* **2003**, *26*, 1424–1427. [CrossRef] [PubMed]
38. Gulcin, I.; Sat, I.G.; Beydemi, S.; Kufrevioglu, O.I. Evaluation of the in vitro antioxidant properties of extracts of Broccoli (*Brassica oleracea*). *Indian J. Food Sci.* **2004**, *16*, 17–30.
39. Badami, S.; Dongre, S.H.; Suresh, B. In vitro antioxidant properties of *Solanum pseudocapsicum* leaf extracts. *Indian J. Pharmacol.* **2005**, *37*, 251–252. [CrossRef]
40. Singleton, V.L.; Orthofer, R.; Lamuela-Raventos, R.M. Analysis of total phenols and other oxidation substrates and antioxidant by means of Folin-Ciocalteu reagent. *Methods Enzymol.* **1999**, *299*, 152–178.
41. Folch, J.; Lees, M.; Sloane Stanley, G.H. A simple method for the isolation and purification of the total lipids from animal tissues. *J. Biol. Chem.* **1957**, *226*, 497–509. [CrossRef]
42. Sasser, M. *Identification of Bacteria by Gas Chromatography of Cellular Fatty Acids*; Technical Note #101; Microbial ID: Newark, DE, USA, 1990. Available online: [http://natasha.eng.usf.edu/gilbert/courses/Biotransport%20Phenomena/pdf/bacteria\\_gc\\_1.pdf](http://natasha.eng.usf.edu/gilbert/courses/Biotransport%20Phenomena/pdf/bacteria_gc_1.pdf) (accessed on 2 January 2022).
43. Tamilselvi, T.; Munish, P.; Jitraporn, V.; Colin, J.B. Evaluation of bread crumbs as a potential carbon for the growth of *Thraustochytrid* species for oil and Omega-3 production. *Nutrients* **2014**, *6*, 2104–2114.
44. Kumaravel, S.; Praveen Kumar, P.; Vasuki, P. GC-MS Study on Microbial degradation of Lindane. *Int. J. Appl. Chem.* **2010**, *6*, 363–366.
45. Lagorce, D.; Sperandio, O.; Baell, J.B.; Miteva, M.A.; Villoutreix, B.O. FAF-Drugs3: A web server for compound property calculation and chemical library design. *Nucleic Acids Res.* **2015**, *43*, 200–207. [CrossRef]
46. Singh, R.; Sahu, S.K.; Thangaraj, M. Polychaete fatty acids as potential inhibitor against human. *Glioblastoma Multiforme* **2013**, *4*, 1519–1524.
47. Reisine, T.; Pasternak, G.W. *Opioid Analgesics and Antagonists.*, in *Goodman and Gilman's: The Pharmacological Basis of Therapeutics*; Hardman, J.G., Limbird, L.E., Eds.; McGraw-Hill: New York, NY, USA, 1996; pp. 521–556.
48. Mossman, B.; Light, W.; Wei, E. Asbestos: Mechanisms of Toxicity and Carcinogenicity in the Respiratory Tract. *Annu. Rev. Pharmacol. Toxicol.* **1983**, *23*, 595–615. [CrossRef] [PubMed]
49. Alan, G.; Porter Reiner, U.; Jae, N. Emerging roles of caspase-3 in apoptosis. *Cell Death Differ.* **1999**, *6*, 99–104.
50. Narayani, S.S.; Shanmugam, S.; Subramanian, B.; Jaganathan, R. Cytotoxic effect of fucoidan extracted from *Sargassum cinereum* on colon cancer cell line HCT-15. *Int. J. Biol. Macromol.* **2016**, *91*, 1215–1223.
51. Porter, D. Labyrinthulomycota. In *Handbook of Protozoa*; Margulis, L., Corliss, J.O., Melkonian, M., Chapman, D., Eds.; Jones & Bartlett: Boston, MA, USA, 1990; pp. 388–398.
52. Dick, M.W. *Straminipilous Fungi: Systematics of the Peronosporomycetes including Accounts of the Marine Straminipilous Protists, the Plasmodiophorids and Similar Organisms*; Springer Science & Business Media: Berlin/Heidelberg, Germany, 2001. [CrossRef]
53. Yokoyama, R.; Salleh, B.; Honda, D. Taxonomic rearrangement of the genus *Ulkenia* sensulato based on morphology, chemotaxonomical characteristics, and 18S rRNA gene phylogeny (Thraustochytriaceae, Labyrinthulomycetes): Emendation for *Ulkenia* and erection of *Botryochytrium*, *Parietichytrium*, *Sicyoidochytrium* gen. nov. *Mycoscience* **2007**, *48*, 329–341.
54. Yokoyama, R.; Honda, D. Taxonomic rearrangement of the genus *Schizochytrium* sensulato based on morphology, chemotaxonomical characteristics and 18S rRNA gene phylogeny (Thraustochytriaceae, Labyrinthulomycetes, stramenopiles): Emendation for *Schizochytrium* and erection of *Aurantiochytrium* and *Oblongichytrium* gen. nov. *Mycoscience* **2007**, *48*, 199–211.
55. Doi, K.; Honda, D. Proposal of *Monorhizochytrium globosum* gen. nov., comb. nov. (Stramenopiles, Labyrinthulomycetes) for former *Thraustochytrium globosum* based on morphological features and phylogenetic relationships. *Phycol. Res.* **2017**, *65*, 188–201. [CrossRef]
56. Leander, C.L.; Porter, D.; Leander, B.S. Comparative morphology and molecular phylogeny of aplanochytrids (Labyrinthulomycota). *Eur. J. Protistol.* **2004**, *40*, 317–328. [CrossRef]
57. Leander, C.; Porter, D. The Labyrinthulomycota is comprised of three distinct lineages. *Mycologia* **2001**, *93*, 459–464. [CrossRef]
58. Plaza, M.; Herrero, M.; Cifuentes, A.; Ibanez, E. Innovative natural functional ingredients from microalgae. *J. Agric. Food Chem.* **2009**, *57*, 7159–7170. [CrossRef]
59. Cote, S.; Carmichael, P.H.; Verreault, R.; Lindsay, J.; Lefebvre, J.; Laurin, D. Non-steroidal anti-inflammatory drug use and the risk of cognitive impairment and Alzheimer's disease. *Alzheimer's Dement.* **2012**, *8*, 219–226. [CrossRef]
60. Guan, L.; Yang, H.; Cai, Y.; Sun, L.; Di, P.; Li, W.; Liu, G.; Tang, Y. ADMET-score—A comprehensive scoring function for evaluation of chemical drug-likeness. *Med. Chem. Commun.* **2018**, *10*, 148–157. [CrossRef] [PubMed]
61. Lipinski, C.A.; Lombardo, F.; Dominy, B.W.; Feeney, P.J. Experimental and computational approaches to estimate solubility and permeability in drug discovery and development settings. *Adv. Drug Deliv. Rev.* **1997**, *23*, 3–25. [CrossRef]

62. Carson, C.F.; Riley, T.V. Antimicrobial activity of the major components of the essential oil of *Melaleuca alternifolia*. *J. Appl. Bacteriol.* **1995**, *78*, 264–269. [[CrossRef](#)] [[PubMed](#)]
63. Bougnoux, P. n-3 Polyunsaturated fatty acids and cancer. *Curr. Opin. Clin. Nutr. Metab. Care* **1999**, *2*, 121–126. [[CrossRef](#)]
64. Rose, D.P.; Connolly, J.M.; Coleman, M. Effect of omega-3 fatty acids on the progression of metastases after the surgical excision of human breast cancer cell solid tumors growing in nude mice. *Clin. Cancer Res.* **1996**, *2*, 1751–1756.
65. Madhavi, N.; Das, U.N. Effect of n-6 and n-3 fatty acids on the survival of vincristine sensitive and resistant human cervical carcinoma cells in vitro. *Cancer Lett.* **1994**, *84*, 31–41. [[CrossRef](#)]
66. Farazi, T.; Leichman, J.; Harris, T.; Cahoon, M.; Hedstrom, L. Isolation and characterization of mycophenolic acid-resistant mutants of inosine-50-monophosphate dehydrogenase. *J. Biol. Chem.* **1997**, *272*, 961–965. [[CrossRef](#)]
67. Bartsch, O.A.; Wagner, G.K.; Hinkel, P.; Krebs, M.; Stumm, B.; Schmalenberger, S.; Bohm, S.B.; Majewski, F. Fish studies in 45 patients with Rubinstein-Taybis syndrome: deletions associated with polysplenia, hypoplastic left heart and death in infancy. *Eur. J. Hum. Genet.* **1999**, *7*, 748–756. [[CrossRef](#)]
68. Shultz, T.D.; Chewa, B.P.; Seamana, W.R.; Luedeckea, L.O. Inhibitory effect of conjugated dienoic derivatives of linoleic acid and  $\beta$ -carotene on the in vitro growth of human cancer cells. *Cancer Lett.* **1992**, *63*, 125–133. [[CrossRef](#)]
69. Newell, M.; Baker, K.; Postovit, L.M.; Field, C.J. A Critical Review on the Effect of Docosahexaenoic Acid (DHA) on Cancer Cell Cycle Progression. *Int. J. Mol. Sci.* **2017**, *18*, 1784. [[CrossRef](#)]
70. Tapieroa, H.; Nguyen, B.G.; Couvreur, P.; Tewb, K.D. Polyunsaturated fatty acids (PUFAs) and eicosanoids in human health and pathologies. *Biomed. Pharmacother.* **2002**, *56*, 215–222. [[CrossRef](#)]